

Rochester Institute of Technology

RIT Digital Institutional Repository

Theses

5-2016

Measurement of Flow Velocities in a To-Scale Simplex Atomizer Using Particle Image Velocimetry

Andrew G. Thistle

Follow this and additional works at: <https://repository.rit.edu/theses>

Recommended Citation

Thistle, Andrew G., "Measurement of Flow Velocities in a To-Scale Simplex Atomizer Using Particle Image Velocimetry" (2016). Thesis. Rochester Institute of Technology. Accessed from

This Thesis is brought to you for free and open access by the RIT Libraries. For more information, please contact repository@rit.edu.

Andy Thistle

Measurement of Flow Velocities in a To-Scale Simplex Atomizer Using Particle Image Velocimetry.

A thesis submitted in partial fulfillment of the requirement for Master of Science in Mechanical Engineering

By Andrew G Thistle

Department of Mechanical Engineering
Kate Gleason College of Engineering
Rochester Institute of Technology
May 2016

Approved By:

Dr. Steven W Day-Thesis Advisor

Dr. Jason Kolodziej

Dr. Michael Schertzer

Dr. Agamemnon Crassidis-Dept. Representative

Acknowledgements:

I would like to thank all of my family, friends and peers who have helped me get this far.

Specifically, I would like to thank my advisor, Dr. Day for taking on a masters project with an application outside of his normal research and for the guidance academically, personally and professionally.

Additionally I would like to thank Advanced Atomization Technologies and RIT for providing the resources for this project. Resources specific to the equipment used for the collection of data were provided by RIT. Other resources specific to the project were provided by Advanced Atomization Technologies. I am grateful for the financial support provided by both parties.

Finally the support provided by Jenifer Bell and my parents, Gay and Harold Thistle provided the drive I needed to complete this project.

Abstract:

To better understand atomization in a commercial aviation gas turbine combustion environment, we present experimental measurements of the internal fuel flow of a simplex atomizer. Particle Image Velocimetry was used to measure velocity in a plane axial to the flow internal to a standard aerospace fuel atomizer. The geometry studied used a 0.74mm orifice and is typical of a commercial aircraft engine. MIL PRF-7024 was employed as the working fluid and two mass flow rates were studied. Particle Image Velocimetry data on a small simplex atomizer was collected and methods are detailed including the machining of the optically clear spin chamber, which properly replicates atomizer geometry, and challenges associated with seeding MIL PRF-7024. The method of data collection is discussed for future application to other geometries. Flow fields showed the majority of mass flowrate around the air core. In addition to increased understanding of this complex flow, this data may be used to support and validate computational analyses of gas turbine fuel injection.

Table of Contents:

Acknowledgements	4
Abstract	6
Table of Content	7
List of Figures	8
Nomenclature	10
Introduction	13
Background	13
How a Simplex Atomizer Works	16
Prior Work	23
Research Gaps	29
Method	31
Results	41
Conclusions	50
References	51
Appendix	52

List of figures:

Figure Number	Description	Page
1	Graphic of a combustor cross section.	17
2	Picture of a modern fuel nozzle	17
3	Gas turbine engine diagram	17
4	Simplex atomizer	18
5	Atomizer assembly diagram	19
6	Atomizer diagram with critical features	20
7	Image of the air core	25
8	Flow field of a large simplex atomizer	26
9	Velocity profile in an atomizer from a computational analysis	27
10	Velocity vectors in a simplex atomizer	28
11	Mass fraction of air in a simplex atomizer, transient analysis	30
12	Typical PIV system	33
13	Test setup	37
14	Atomizer imaging setup	38
15	Test article	39
16	Imaging focusing exercise	40
17	Particles	41
18	Velocity profile data taken at 5 μ s and 10 μ s	45
19	Velocity profile data taken at 30 and 90 psi	46
20	Velocity vectors taken at 30 and 90 psi	46
21	Data range at an axial location	48
22	Atomizer swirl plug assembly dimensions	53

Table of Tables:

Table Number	Description	Page
1	Research gaps	32
2	PIV equipment	35
3	Mass flow vs. pressure	37
4	Nominal atomizer dimensions	52

Nomenclature:

PIV	Particle Image Velocimetry
JetA	Universal fuel used in commercial aviation
CO	Carbon Monoxide
NOX	Nitrogen based pollutant
°K	Degrees Kelvin
\dot{m}	Mass Flow
n	number of holes in swirl plug
β	Hole angle
D_c	Spin chamber diameter
d_o	Orifice diameter
D	plug hole diameter
u	Axial Velocity
v_i	Tangential Velocity
ρ	Density
FN	Flow Number
X	ratio of air core area to orifice area
P	axial pressure
A_o	Orifice Area
A_a	Air Core Area
C_d	Discharge coefficient
R_s	orifice offset

t	film thickness
LPV	Laser Particle Velocimetry
σ	surface tension
ν	kinematic viscosity
μ	dynamic viscosity
Re	Reynolds number
We	Weber number
G&M	Giffen and Muraszew
ALE	Arbitrary Lagrange Eularian
CFD	Computational Fluid Dynamics
VOF	Volume of Fluid
LDV	Laser Doppler Velocimetry
MIL-PRF-7024	A calibrated fluid used for testing when JetA is unsafe
nm	nanometer
WIDIM	Window Deformation Iterative Multigrid
kPa	Kilo Pascal
$\frac{kg}{h}$	Mass flow rate kilograms per hour (SI)
PPH	Mass flow rate Pounds per hour (English)
Tween 20	A surfactant brand name
μm	micrometer
u_o	Fluid velocity
l_o	Characteristic length

Andy Thistle

ρ_d	Particle density
d_d	Particle diameter
μ_g	Viscosity of fluid
Stk	Stokes number
t_0	Stokes number time constant

Introduction:

In this work an experimental analysis using Particle Image Velocimetry (PIV) is used to collect velocity field data internal to a simplex atomizer. Velocity field data can be used to build and validate a numerical model of the fuel flow inside of an atomizer, and the fuel flow as it leaves the atomizer and is burned. Measurement error is analyzed and provided to quantify measurement discrepancies. Simplex atomizers, machines used to create a fine mist of liquid droplets, are commonly used in gas turbine applications to inject liquid fuel due to simplicity, effectiveness and lack of moving parts. Atomization in a simplex atomizer relies on surface tension to break a continuous flow into small droplets. The geometry of the atomizer plays a key role in the quality of the spray. A typical aerospace application requires a relatively small atomizer, which have not been the subject of past PIV studies. For numerical models of fuel injection in gas turbine engines to be viable design tools, the models must be validated with experimental data. This research provides experimental data and methods that can be used to accurately validate numerical models. The small size introduces challenges to the PIV measurement technique, but requires no assumptions in regards to fluid scaling. The working fluid in this experiment has very similar properties to JetA and an optimal index of refraction.

Background:

The advent of the aerospace gas turbine engine brought about a race for performance and efficiency, both for military superiority and economic advantage. In military applications efficiency equates to an increase in aircraft range or thrust, in commercial aviation applications the motivation is increased range and lower fuel costs. The gas turbine engine is a Brayton cycle engine (Figure 3), which has a direct relationship between higher efficiency and increased

average temperature. Recently emissions have been an additional consideration. Pollutants formed in a gas turbine engine are generated in the combustor (Figure 1) and are based on complicated combustion dynamics that are very sensitive to subtle variations. Nitrous oxide and carbon monoxide (CO) are the pollutants of most concern. Nitrous Oxide (NO_x) is generated at a significant rate when combustion temperatures exceed 1850 K (Lefebvre and Ballal 2010). To minimize NO_x emissions generally the flow is quenched by cooler air, but at the cost of incomplete combustion, and CO creation. Optimally the fuel would be stoichiometrically mixed allowing the combustion to occur in a 'diffuse' flame and the temperature to be evenly dispersed throughout the flow. Liquid fuel poses even more difficulty because the droplets must evaporate before burning. Many local hot spots are created as droplets vaporize and burn; these facilitate the formation of NO_x. Although many different techniques are being investigated for creating an even, diffuse flame in a gas turbine combustor, the current method is to atomize the fuel in a consistent small droplet size range into a sector of the combustor. The fuel nozzle accomplishes this and must be better understood in order to consistently meter a fine mist of fuel. A modern fuel nozzle is pictured in Figure 2.

The ultimate goal in atomizer design is to understand the relationships between internal nozzle flow and the combustor, linking emissions with the atomizer and fuel system. A model with this degree of resolution would allow a significant reduction in emissions from gas turbine engines. With increased computational power or efficiency this type of model could be iterated in order to arrive at an optimized atomizer and fuel system design. As progress is made in computing power and direct numerical simulations of atomizing sprays, the need for data on the fluid structure internal to the atomizing mechanism arises (Benjamin, Jensen et al. 2010). Experimental data internal to the fuel nozzle will provide initial condition and baseline data for

flow models that can be inserted into larger simulations of gas turbine engine combustors. The advent of such a model would allow new engines to be developed faster with higher efficiencies and lower emissions.

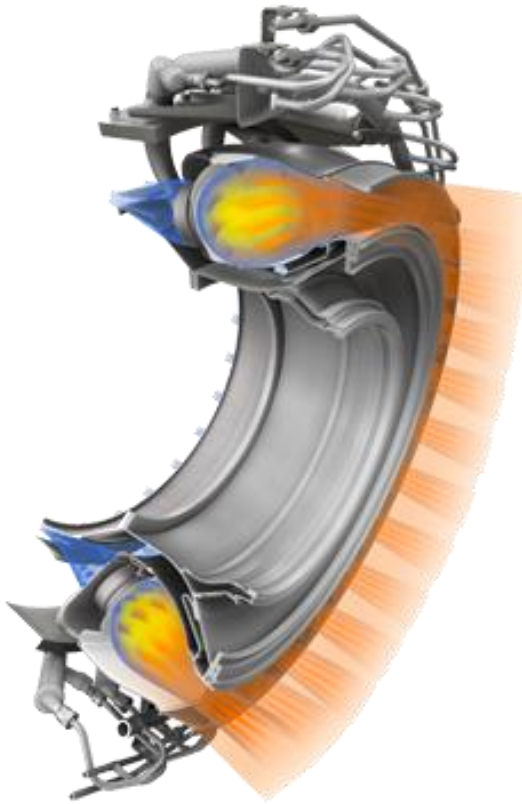


Figure 1: A modern combustor design with fuel nozzles showing airflow and combustion. (CFM 2016)



Figure 2: A fuel nozzle (GE 2014)

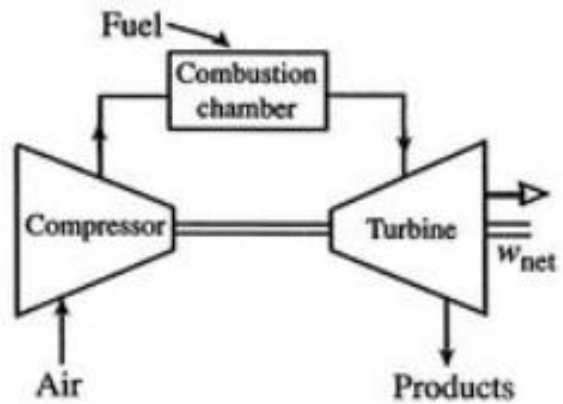


Figure 3: A diagram of a gas turbine engine. The combustor section is shown in Figure 1. (MIT 2016)

How it Works:

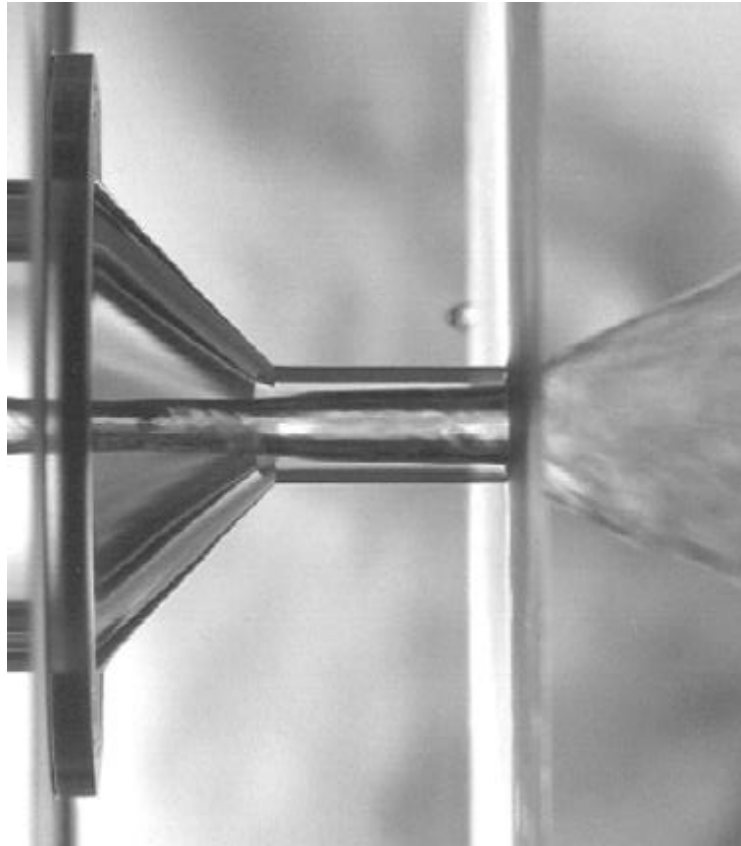


Figure 4: A simplex atomizer showing the air core, fluid passing through the orifice and forming a thin cone. (Steinthorsson, Ajmani et al. 1997)

A simplex atomizer works by imparting a swirl in a fluid (in this case imparted by the swirl plug Figure 5), forcing the fluid to form a thin film on the inner diameter of a cone, which is the primary body. The direction of rotation is driven by the direction of the ports on the swirl plug. The layer of fluid is necked down, increasing axial velocity through the orifice (Figure 4 and 5). Upon exiting the atomizer the fluid forms a conical sheet which thins as the sheet expands, until the cone succumbs to the forces of surface tension, disintegrating into many small droplets. This creates a fine mist desirable for combustion. The dimensions of the atomizer

studied are detailed in Table 4 (appendix). The radial velocities internal to the atomizer are large enough to create a hollow air core in the center of the atomizer. This fluid-fluid boundary adds complexity to the flow within the atomizer and further complicates the PIV measurement.

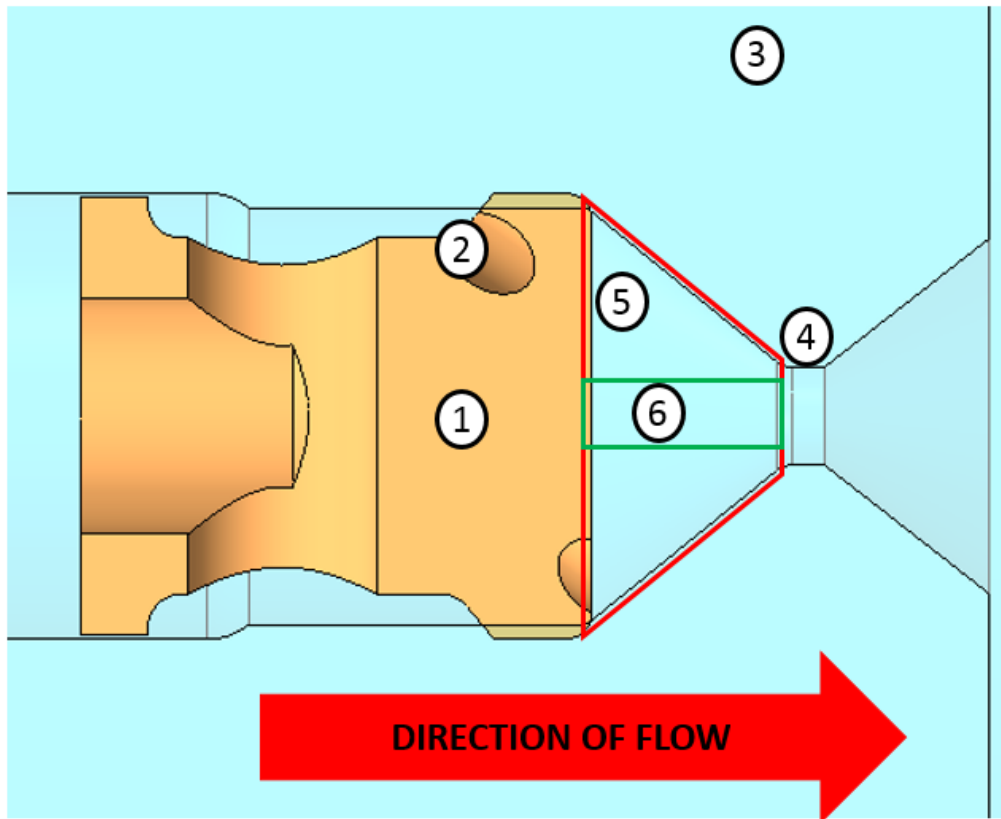


Figure 5: Test geometry sectioned through the axis of rotation of the fuel. The fluid rotational component is large enough to create a low pressure zone along the axis of rotation which fills with air.

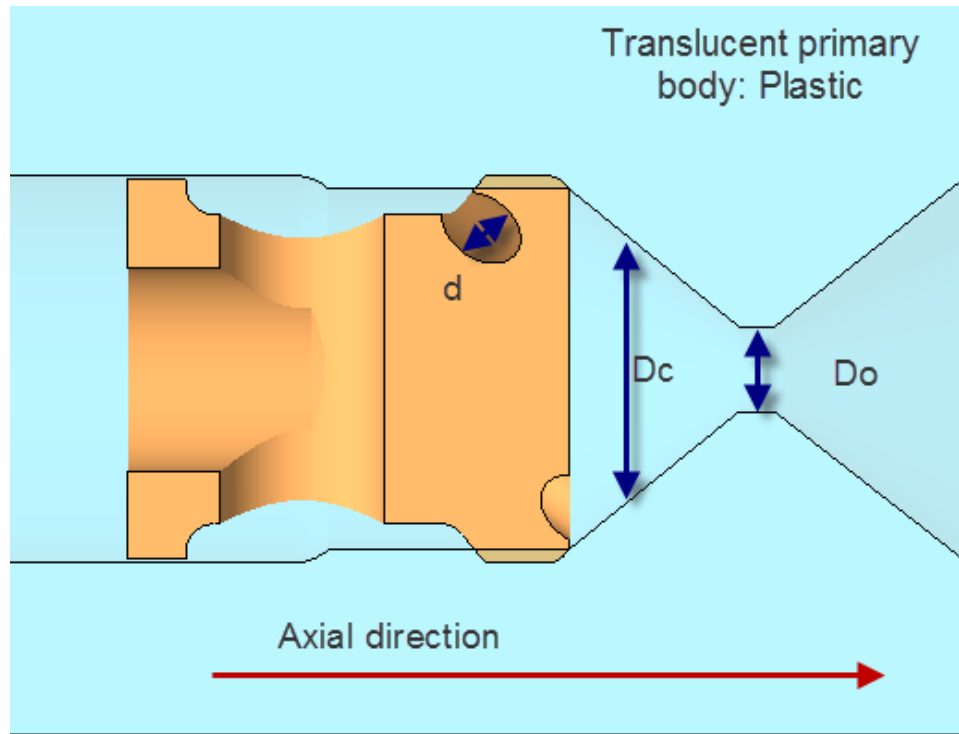


Figure 6: Geometric parameters of consideration in a simplex atomizer

A simplex atomizer works by imparting a rotational component to the flow and forcing it through an orifice along the axis of rotation. Figure 5 describes the atomizer design used in this research. The design employs two parts; a swirl plug (pictured in peach see Figure 5) and an orifice body. The pictured design allows ease of manufacture. The rotational component of the flow is imparted by 3 holes drilled at an angle and offset from the centerline of the part. A simple inviscid 1D mass flow analysis of a simplex atomizer leads to the following equations describing the flow velocities within the system. The equations describing the flow are rudimentary, but serve to estimate maximum flow velocities within the atomizer.

Andy Thistle

\dot{m} =Mass Flow

n =number of holes in swirl

plug

β =Hole angle

D_c =Spin chamber diameter

d_o =Orifice diameter

d=plug hole diameter

u=Axial Velocity

v_i =Tangential Velocity

ρ = density

FN=Flow Number

X=ratio of air core area to
orifice area

P =axial pressure

A_o =Orifice Area

A_a =Air Core Area

Cd =Discharge coefficient

R_s =orifice offset

t =film thickness

$$FN = \frac{\text{Flow rate}}{\sqrt{\text{pressure differential}}} \quad (\text{Lefebvre 1988})$$

Flow number (FN above) is commonly used to describe simplex atomizers, because the atomizer is the largest pressure drop in a typical simplex atomizer system. As a quasi-nondimensional parameter flow number allows flow rate or pressure drop to be scaled assuming incompressible and inviscid flows. Applying the conservation of momentum equations yields the following two equations.

$$vr = v_i R_s \quad (\text{Lefebvre 1988})$$

$$V = \frac{\dot{m}}{\rho \pi d^2 n}$$

$$u = V \sin \beta$$

$$v_i = V \cos \beta$$

$$P = \frac{1}{2} \rho (u_{r_a}^2 + v_{r_a}^2) \quad (\text{Lefebvre 1988})$$

$$u = \frac{\dot{m}_L}{\rho_L (A_o - A_a)} \quad (\text{Lefebvre 1988})$$

The above equations describe velocities based on an inviscid conservation of mass analysis. In the proposed work the atomizer to be analyzed uses angled flow slots instead of

fully tangential inlets. Therefore the axial velocity is not solely pressure driven. This geometry is unique to LPV based research on simplex atomizers, it is predicted the flow will be more unsteady in nature. To ensure the flow velocities are properly captured the inlet flow must be broken into respective vectors as shown above. Dimensions associated with the air core were backed out of experimental analysis and are shown below. From Lefebvre:

$$Cd = (1 - X) \quad (\text{Lefebvre 1988})$$

$$X = \frac{(d_o - 2t)^2}{d_o^2} = \frac{A_a}{A_o} \quad (\text{Lefebvre 1988})$$

The above equations provide 1D flow data on atomizer performance, which is not sufficient for atomization numerical models or design tools. The highly rotational flow retards the formation of a boundary layer, and inhibits the development of turbulent flow (Lefebvre 1988). Reynolds number is defined as the ratio of inertial forces in the flow to viscous forces.

σ =surface tension

ν =kinematic viscosity

μ =dynamic viscosity

Inertia/viscous
Reynolds number

$$Re = \frac{\rho VL}{\mu} = \frac{VL}{\nu}$$

Andy Thistle

Ma, (Ma 2002), presents evidence that the flow inside a simplex atomizer does exhibit turbulent characteristics, but other research documented in his work attributes similar effects to a fluctuating air core.

A second non-dimensional parameter that pertains to the proposed work is the Weber number. The Weber number is the ratio of inertial forces to surface tension forces and is commonly used in analysis involving droplet formation (Robert W. Fox 2011).

$$\begin{array}{l} \text{Inertia/surface tension} \\ \text{Weber number} \end{array} \quad We = \frac{\rho V^2 L}{\sigma}$$

While Weber number is only relevant at the fluid-fluid boundaries such as the air core and the exit of the orifice, there is some speculation that it plays a greater role in the internal flow field as well. In this particular experiment the small size of the atomizer being tested could amplify the effects of viscous and surface tension forces.

Prior Work:

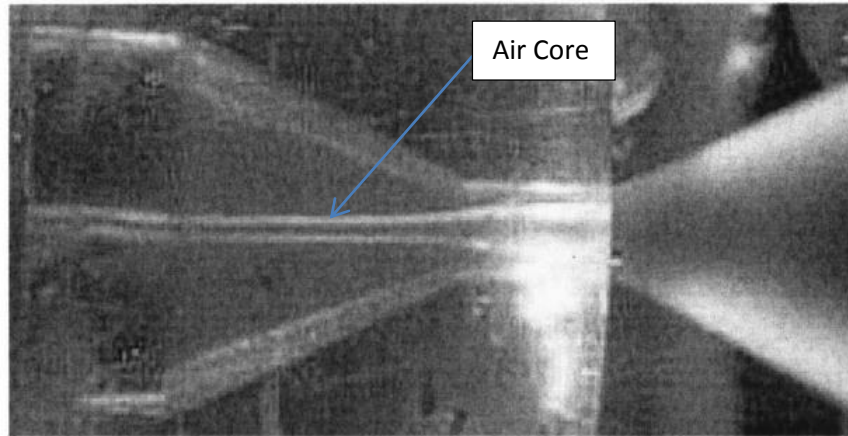


Figure 7: A photograph of the air core in a translucent simplex atomizer. (Dash, Peric et al. 2001)

The need for consistent simplex atomizers has driven vast amounts of research into the field. Past research into flow fields in simplex atomizers have been focused on large diameter orifices and idealized atomizer designs. For example, in previous research, mathematical characterization of the air core was performed by (Dash, Peric et al. 2001)). A Navier-Stokes based approach was employed to mathematically identify the fluid-fluid boundary. The empirical model was validated by photographing the air core (Figure 7) and comparing geometries. Unsteady fluctuations in the air core mathematical model matched experimental observations, although the experimental method was not sophisticated enough to provide conclusions beyond visual comparison.

Early research yielded inviscid flow models for the design of simplex atomizers that are still used and are based on fundamental fluidics and vast amounts of experimental data.

Collected data was compiled into curves describing scaling factors at different flow conditions and varying geometries. Subsequent research has focused both on experimental and empirical modeling of simplex atomizer systems. Refinement of the inviscid models presented by Giffen and Muraszew (Lefebvre 1988) (G&M) was attempted by (Xue, Jog et al. 2004)). Xue used an Arbitrary Lagrange Eularian (ALE) Computational Fluid Dynamics (CFD) model, anchored by data taken using Laser Particle Velocimetry (LPV) to expand upon the curves developed by G&M. A single 21 mm orifice diameter atomizer with interchangeable geometries was employed in the experimental analysis. The resulting model (predicted flow field shown in Figure 8) proved more accurate than those developed by G&M, however the improved model was focused on larger orifices and specialized geometry. Ideally, a design tool would accommodate a wide range of geometries.

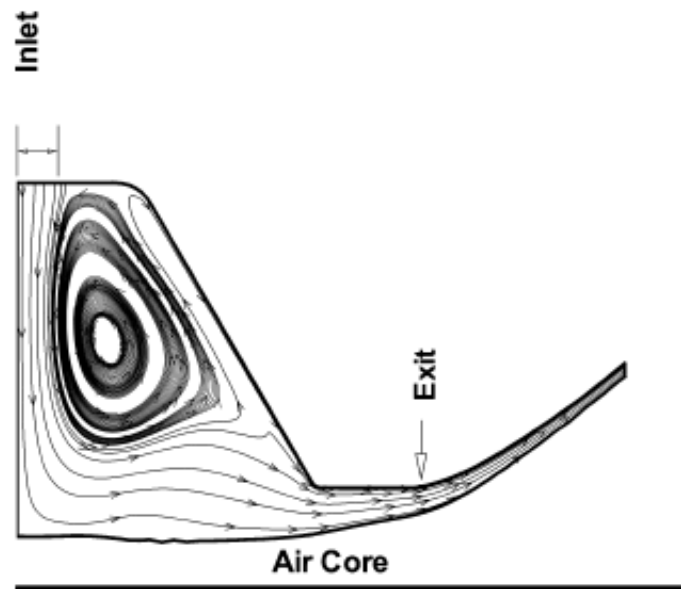


Figure 8: Xue et al. A flow field of a large simplex atomizer as calculated using an ALE numerical method.

The data collected in similar experiments was used by (Steinthorsson, Ajmani et al. 1997)) by employing a Volume Of Fluid (VOF) CFD technique. CFD models are challenged by

simplex atomizers by the fluid-fluid interactions of the air core, which can be unsteady, and the turbulent swirling flow. There is also the opportunity for non-isentropic conditions at the boundary. This CFD technique was seen as relevant due to its creative means of maintaining a very dynamic fluid-fluid boundary such as the air core. The model maintained separate meshes for each fluid, and calculated the interface geometry. Periodically the interface was recalculated in order to maintain model fidelity. The technique was also able to be implemented in the commercially available software Fluent. The flow field, film thickness and air core geometry modeled correlated well with experimental data. The velocity profile near the exit plane is shown in Figure 9. A peak in swirl velocity centered around the air core was not captured when compared to experimental data, and the overall pressure drop through the nozzle was significantly higher because of this. Although CFD techniques better capture local flow phenomena and are not limited by size further investigation was required to refine this method. Future work could employ an unsteady large eddy simulation or direct numerical simulation, but these simulations were determined to be not economical at that time.

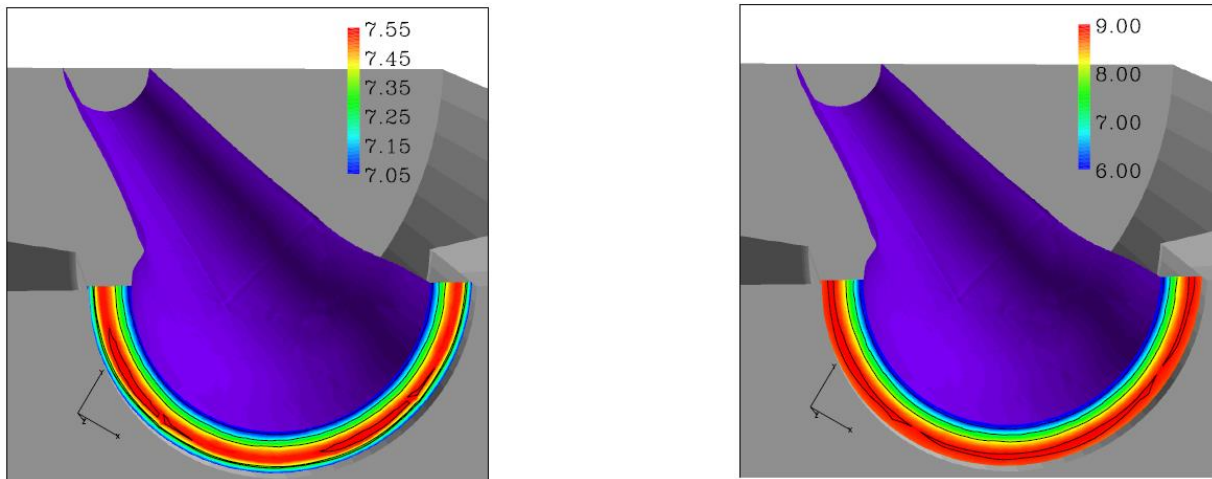


Figure 9: Steinthorsson et al. Velocity profiles 1 mm (.039") from orifice exit plane. Axial velocity shown on the left and tangential velocity on the right.

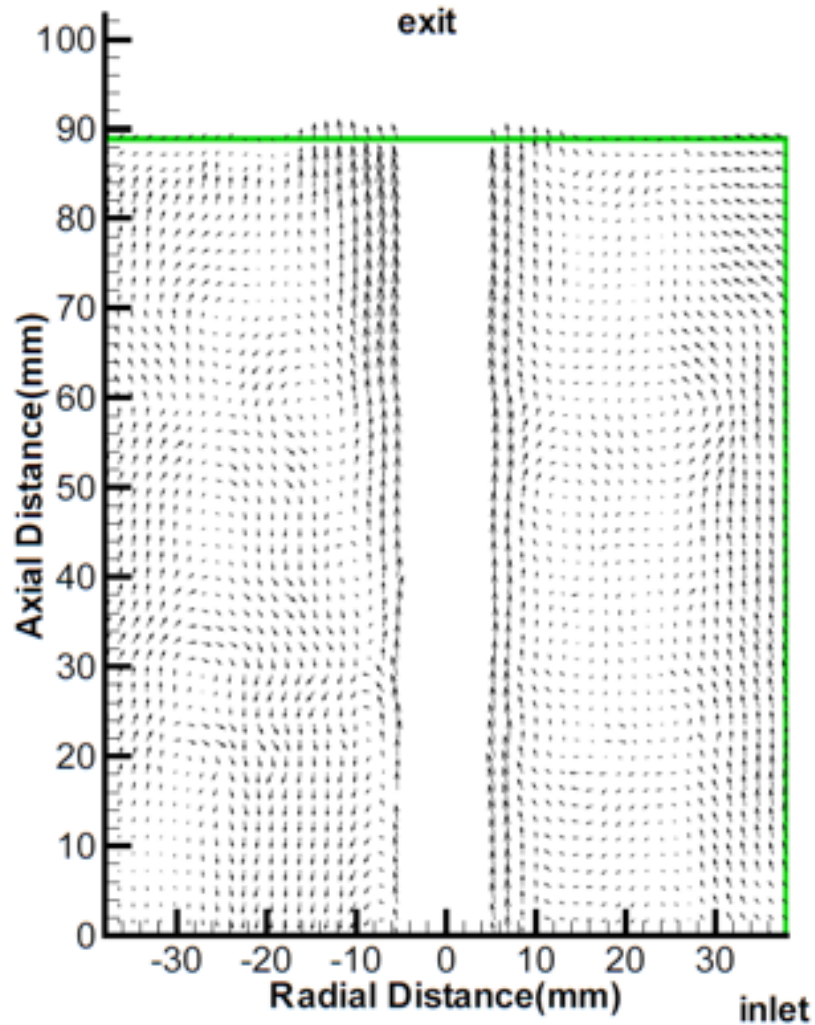


Figure 10: Ma et al. LDV data bisecting the air core of a simplex atomizer. Note the large majority of mass transport shown along the air core.

Laser Doppler Velocimetry (LDV) and LPV were employed by (Ma 2002)) in an experimental study into geometries of varying size above 1 mm (.039"). Ma focused on identifying the effects of internal geometries on simplex atomizer performance as well as the classification of the flows within the atomizer. His research employed two separate methods of data collection in order to validate his findings. Correlation data showed the dissimilar methods

gathered comparable data further validating the technique. Imaging was performed in a plane bisecting the air core and in a plane normal to the air core (Figure 10). The study resulted in more accurate relationships between geometry and flow characteristics inside a simplex atomizer. Furthermore, Ma concluded that the flow observed inside the large scale atomizer was turbulent. In this study Reynolds number was scaled, however other unsteady effects such as Weber's number were not.

(Baharanchi, Florida International University et al. 2013)) tested four purely empirical flow models of simplex atomizers offered in the commercially available software package Fluent. The models differed in the interface calculation schemes, the methods vetted were Implicit, Euler-Explicit, Geometric-Reconstruction and Donor-Acceptor. They concluded that a combination of local adaptive mesh refinement and Geometric-Reconstruction was superior. All

methods evaluated correlated within 10% of available velocity field data from the research

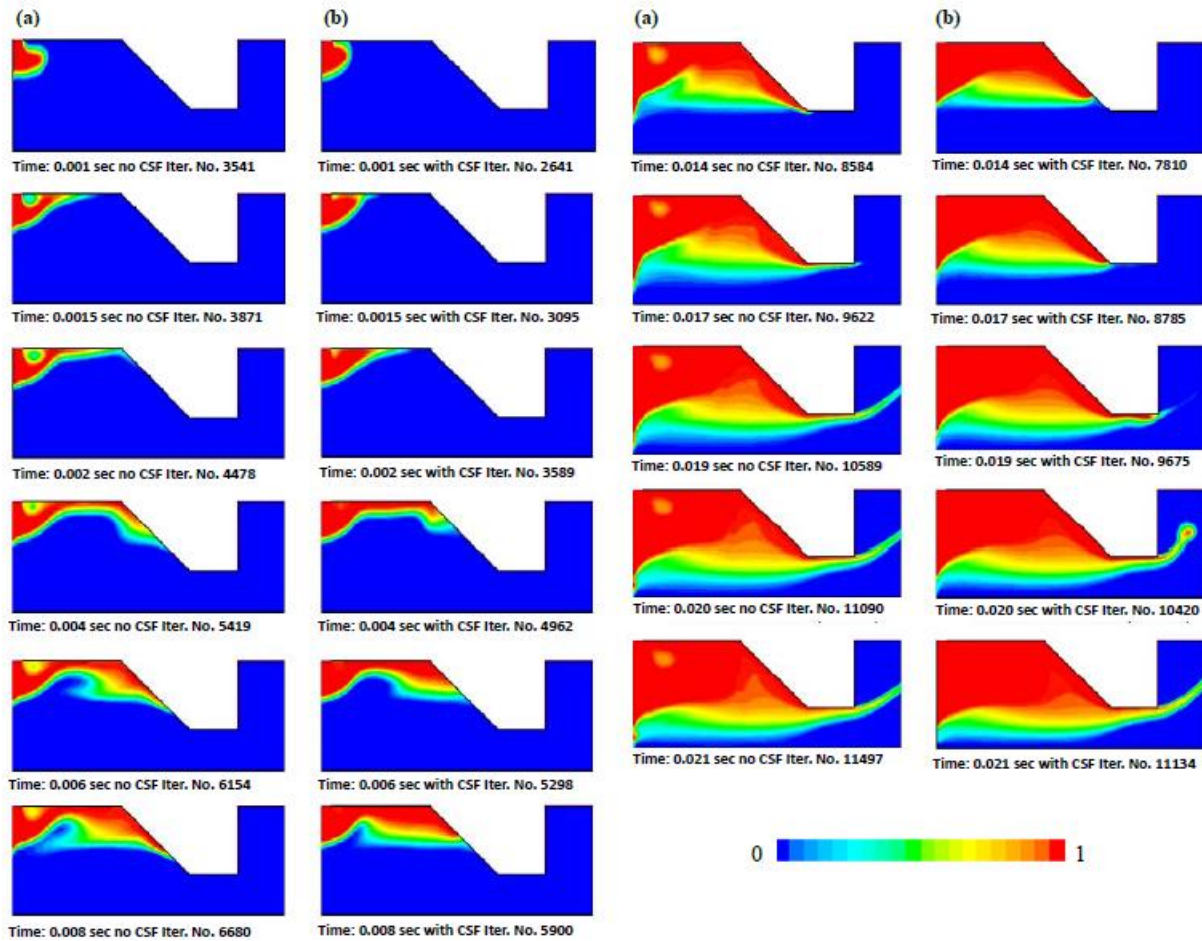


Figure 11: Transient plots of mass fraction of air for a model with and without Continuum Surface tension Force (CSF). Blue represents air. A significant influence on flow development by surface tension can be observed.

performed by Ma. Steady state and transient conditions were analyzed as well, but there was no available data on the transient flow. In addition to evaluating the effectiveness of 4 interface calculation schemes the research sought to determine a threshold Weber number where surface tension effects merit the inclusion of a continuum surface tension force. The transient models (Figure 11) run with and without the surface tension force showed that it was relevant in flows greater than 1 m/s correlating with a Weber number of 204. This is not a high velocity or weber number for this type of flow. In the transient velocity plots it can easily observed that surface

tension forces have a heavy influence on the flow development, and the steady state data also shows error if the forces of surface tension are neglected.

In the future, research into spray atomization will require increasingly complex models thus demanding more computational power. Breakup analysis, focusing on the flow immediately after exiting the nozzle is integral to improving efficiencies and emissions going into the future (Benjamin, Jensen et al. 2010). The near nozzle region loosely defined as the spray cone from the exit of the atomizer to about 5mm (0.2”) downstream is extremely complex to model and measure. Typical measurement methods employed internal to the atomizer or in the downstream spray are unable to measure within the dense near nozzle region. Without the ability to model the near nozzle region combustion modeling must rely on statistical models regarding fuel spray. These models cannot provide the fidelity needed to properly understand and design for pollutant formation. Understanding the internal flow of the atomizer will improve the ability to model near nozzle flows.

Research gaps:

Quantitative velocity data: The majority of past research into spray atomization focuses on statistical droplet modeling downstream of the injector. For a comprehensive understanding of the physics of atomization near nozzle and internal fluid flow must be understood. The limited research into internal flows can be characterized into experimental studies and computational models. Computational models must rely on experimental data to verify results, and are limited by computing power. Advances are brought about by implementing algorithms that more efficiently utilize computational resources. These models must be verified by quantitative experimental data. Experimental analysis on simplex atomizers has been greatly

advanced through Particle Image Velocimetry (PIV) and LDV. These two techniques allow flow fields to be quantified for analysis and comparison.

Atomizer size: In order to develop highly generalized relationships, past research has been focused on very large geometries with exaggerated spin chamber size. Ma , Xue et al and Wang et al provide flow field data on simplex atomizers, but with orifices ranging from 11 to 21mm (0.433”-0.826”) as opposed to the .74 mm (0.029”) orifice studied here (Table 1). These characteristics allow a large measurement area. There are applications for simplex atomizers with large orifice diameters and past research on large scale atomizers have properly scaled test conditions using Reynolds number. However Weber’s number and density ratio, between the working fluid and the atmosphere, scaling was not taken into account.

Fluid properties for imaging: The working fluid in some past research has been water. Water has a very different index of refraction than the plastic atomizer, limiting the measurement area to a location where the laser sheet can make the transition from plastic to working fluid along a normal surface.

Author	Analysis type	Atomizer size
Ma, 2002	Experimental (PIV, LDV)	11-21 mm (.433-.826 in)
Xue et al, 2004	Experimental (PIV) Empirical (CFD)	21 mm (.826 in)
Wang et al, 1999	Experimental (PIV, LDV)	11-21 mm (.433-.826 in)
Thistle	Experimental (PIV)	.74 mm (.029 in)

Table 1: Studies of flow field data using simplex atomizers. Note that the .74 mm (0.029”) orifice used in this study is much smaller than those studied previously.

The working fluid used was mil-prf-7024, a mineral oil based fluid with similar properties as jet fuel. Mil-prf-7024 has a similar index of refraction as optical Plexiglas and is commonly used in experimentation focused on spray atomization.

Method:

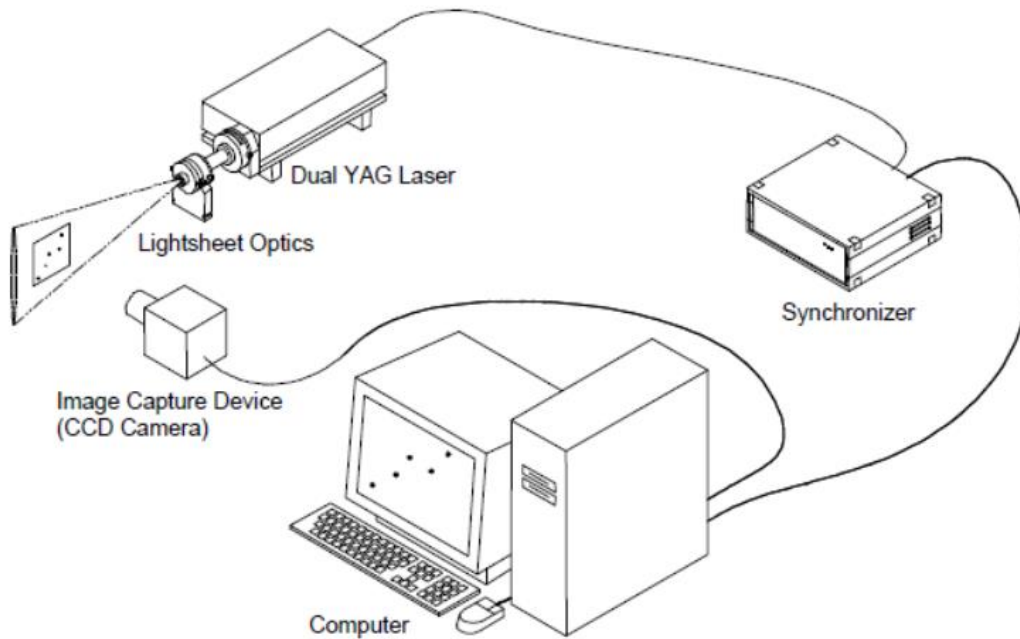








Figure 12: A typical Particle Image Velocimetry (PIV) system. The synchronizer and computer serve to coordinate the laser and the camera. The camera uploads images directly to the computer to be processed later. (1997)

The method presented is an experimental analysis using Particle Image Velocimetry (PIV). PIV is an experimental fluidics technique relying on image pairs to gather a flow field of a targeted sample. The key components of a PIV system are a laser, a high speed camera and circuitry to coordinate the laser illumination with the camera (Figure 12 and Table 2). The laser system contains two discrete lasers in order to fire rapidly in pairs. The camera must be capable of exposing a separate frame during the individual laser pulses and must be tailored to gather data in a very short period of time. The circuitry must coordinate the two systems. The sample rate is based on the flow velocity; high speed flows require more rapid sampling. A laser illuminates a 2D plane within a fluid while simultaneously taking a picture. Immediately a

second frame is exposed, and a second laser pulse follows at a dictated time. The laser is powerful enough to saturate the image with a 1 meter burst capturing the particles over approximately 8 nanoseconds, this is 3 orders of magnitude faster than the shortest time between frames. Image pairs are taken many times a second. The result is still frames depicting the location of seed particles at a certain time. Within the time between frames, the particles have either translated or rotated. The patterns formed by groups of particles are analyzed statistically. Displacement is quantified and combined with many other data points to yield a flow field (Raffel, Willert et al. 2007). Due to the reliance on optics, consideration must be made as to materials, working fluid and seed particles. Materials must be optically clear and must match index of refraction very closely with the working fluid. Seed particles must be neutrally buoyant to provide accurate flow measurements, yet they also must be visible to the camera. In this experiment the seed particles fluoresce red, while the laser is operating at 532 nm which is green. This allows the laser light to be filtered from the camera, but still allows the relevant particle location data to be collected.

The Particle Image Velocimetry (PIV) system was a TSI (brand) system employing Insight 3G for data acquisition and post processing. The atomizer was kept stationary, while the optics were mounted on a periscope assembly. This allowed fine adjustment of the imaging plane. The components of the PIV system are shown in Table 2.

PIV System			
Function	Make	Model	
Laser	New Wave Research	Solo 200XT 15Hz	 
Camera	TSI	PIVCAM 13-8	
Lens	Cannon	MP-E 65mm f/2.8 1-5x Macro Photo Lens	
Synchronizer	TSI	Laser Pulse	 
Computer/software	Dell running Windows XP	Insight 3G software	

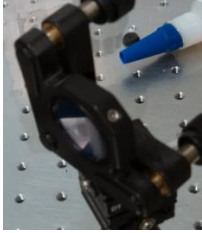
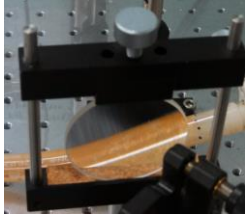
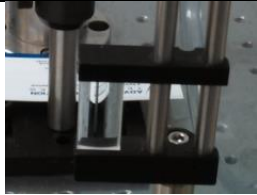
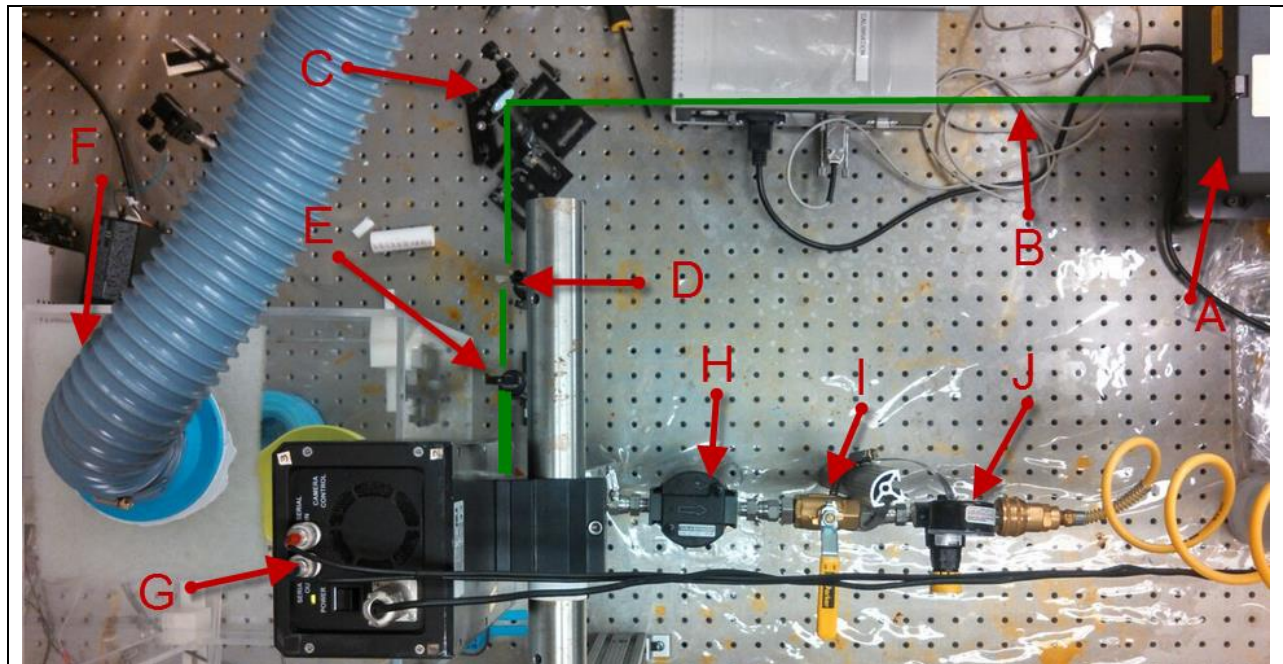
Mirror	Thor Labs	532nm reflective	
Spherical lens	Edmund Optics		
Cylindrical lens	Thor Labs		

Table 2: Equipment in PIV system.

Images taken with the TSI system were processed in a Matlab script titled PIV_Processing (Zeller, Jayasekera et al. 2014) in order to convert the image format to one friendly with the PIV software. A second Matlab script titled PIV_Post_Processing (Zeller and Jayasekera 2014) called the program WIDIM (Window Deformation Iterative Multigrid) software (Scarano 2001) and iterated through the desired image pairs. WIDIM produced velocity vectors from the images which are discussed in the results section.



A	LASER HEAD
B	UNFOCUSED PULSED LASER BEAM PATH
C	MIRROR 45° FROM BEAM PATH
D	CYLINDRICAL LENS, SPREADS BEAM INTO A SHEET
E	SPHERICAL LENS, COLUMNATES SHEET TO CONSISTANT PLANE AND FOCUSES THICKNESS
F	VENTED BOX, ROOM PRESSURE VENTED TO THE OUTSIDE
G	CAMERA
H	RESERVIOR
I	BALL VALVE
J	PRESSURE REGULATOR

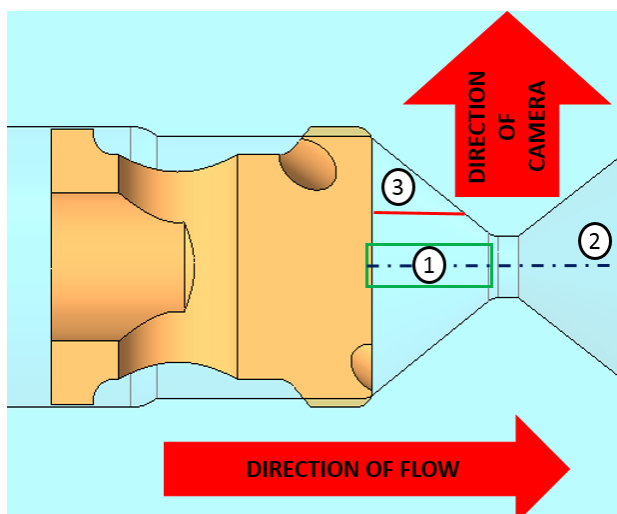
Figure 13: Test setup, laser path is seen in green.

The layout of the PIV system can be seen in Figure 13. Image pairs were taken with a set time between exposures based on the 1D calculated flow velocities, but time was not held constant between image pairs. The flow in a simplex atomizer poses challenges to PIV measurement due to the high rotational velocities. The swirl in the atomizer causes the particles to rapidly move in and out of the plane of measurement. Many particles are captured in one frame and are absent in the next, producing no PIV data. A cannon 65mm macro lens was paired with the camera in order to maximize the number of pixels inside the spin chamber. The macro lens allowed a resolution of 7.7 pixels per .025 mm (0.001”).

The atomizer assembly was plumbed to a pressure transducer and the fluid reservoir (Figure 13). The system was designed to plenum feed the atomizer in order to best control the mass flow rate. During the data collection the pressure was controlled by a regulator on the air line. This air pressure regulator and a ball valve were used to control the flow and were placed upstream prior to the reservoir. This limited the fluid exposure to the pressurized air to the approximately 40 s it took to empty the reservoir. The atomizer exited into a tube in order to maximize fluid recovery. The tube was contained in an acrylic box that was ventilated to the outside. Mass flow of the atomizer was calibrated with relation to pressure, and the pressure was controlled by a regulator on the air line. Flow rates at each pressure point are shown in Table 3.

Flow rates		
Pressure kPa (psi)	Mass Flow kg/h (PPH)	FN (-)
207 (30)	8.47 (18.68)	3.4
621 (90)	14.65 (32.3)	3.4

Table 3: Mass flow vs. pressure. Data taken at the AATech facility. PIV measurements controlled pressure without measuring flow.



The experiment employed a simple atomizer conventionally machined from optically clear acrylic with a metal swirl plug pressed into the acrylic. The acrylic was chemically conditioned in order to remove machining marks and ensure an optically transmissible surface. The imaging plane was

Figure 14: Atomizer geometry perpendicular to the camera. 1) The air core. 2) The centerline of the flow. 3) Laser sheet defining the imaging plane.

offset from the orifice centerline by 1.0 mm (.040") (Figure 14 and 15), and data was processed for points in between the orifice and the swirl plug. This offset imaging plane

shows axial as well as rotational data and prevents interference from the fluid-fluid

boundary of the air core. PIV is only sensitive to the velocity within the imaging plane, so the offset of the imaging plane served the function of collecting data with a rotational component.

The atomizer geometry has a flow number of 3.4. The dimensions of the test section are shown below in Table 4 (appendix). Data was processed for points in between the orifice and the swirl

plug (Figure 14). This research is limited to a single plane. In order to set the imaging plane, a 0.3175 mm (0.0125 in) tube was fed into the orifice (Figure 16) this set up a centerline that could be used as a measurement reference. The spin chamber was filled with fluid allowing the camera to be focused and the laser to be aimed at the tube (Figure 16). The orifice was blocked during this process so that the fluid was stagnant. The fluid having the same index of refraction as the acrylic allows an undistorted view of the tube. The laser was then adjusted to illuminate the tube and this was set to zero. Once the laser was zeroed it could be offset a set dimension, in this case 1.0 mm (.040") to capture the desired measurement plane.

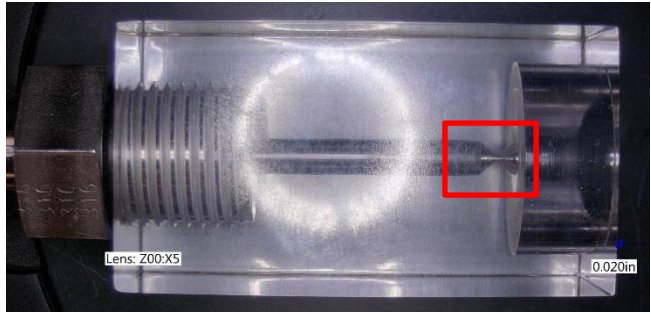


Figure 15: Test article. The box encloses the area depicted in Figure 14

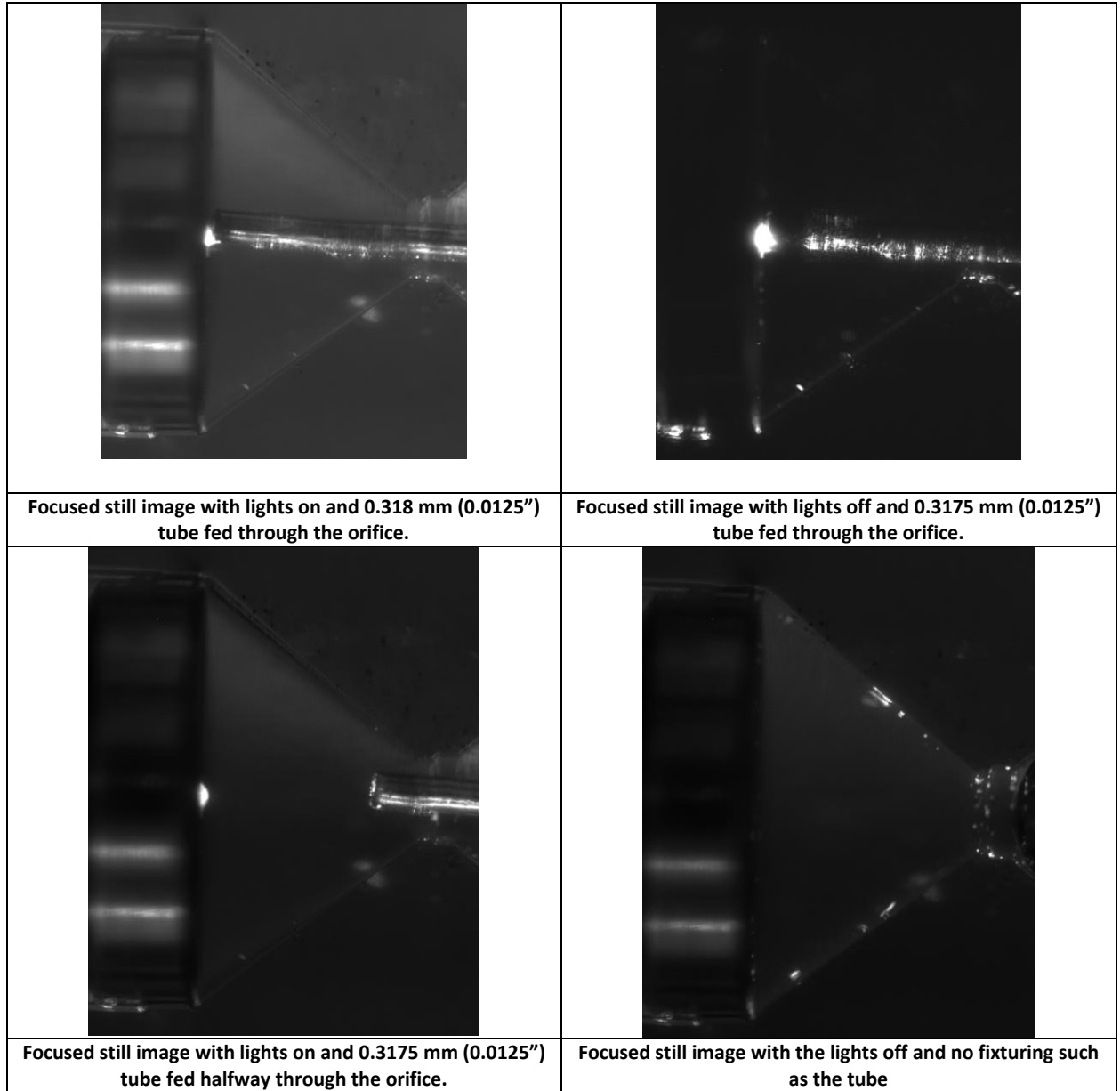


Figure 16: A 0.3175 mm (0.0125") tube was used to focus on the center plane of the atomizer. The tube was then removed and the laser offset to set the imaging plane.

The fluid in this experiment was MIL-PRF-7024, or calibration fluid, with a surfactant, Tween 20[®], for better particle suspension. Calibration fluid is commonly used as a test fluid in lieu of Jet A because of the higher flash point and equivalent viscosity of the calibration fluid. Additionally, the index of refraction of the calibration fluid matches the acrylic primary body. Polystyrene particles mixed into calibration fluid quickly fall out of suspension and aggregate at the bottom of the container. The addition of a small amount of surfactant proved somewhat

effective in preventing this sedimentation. The successful solution consisted of 200ml calibration fluid with the addition of 1% Tween 20[®] surfactant, and 10 μ m polystyrene spheres to give sufficient particle fill. Some particles continued to fall out of suspension and additional particles needed to be added. The fluid required agitation until immediately before atomization in order to minimize particle sedimentation. The mineral oil based calibration fluid did not affect the particles chemically, but there was a miscibility issue. The solution had to be refreshed with particles often, due to the particles aggregating on surfaces.

Initially no surfactant was used in the solution, the particles adhered to each other and aggregated at the bottom of the solution. The particles used were tailored for denser solutions

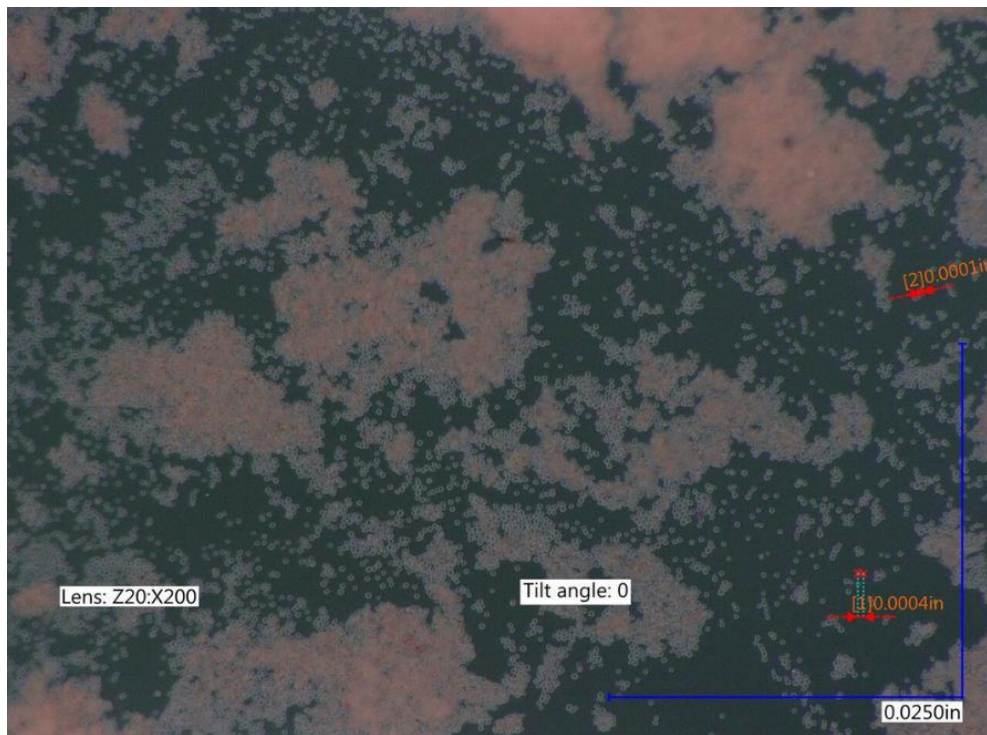


Figure 17: 9 μ m beads shown at 200X when mixed with mil-prf-7024. Notice the majority of the beads have adhered to each other and have fallen out of suspension, but the beads maintain their form and function.

and were not completely miscible with the mil-prf-7024. Evaluation under a microscope in Figure 17, showed the particles retained their shape and

fluorescent dye. Initially the addition of .2% Tween 20[®] to the solution and agitation was tried with some success. Additional Tween 20 was added with increasing effectiveness until a concentration of about 1%, after which no improvement was observed. The solution required agitation, and after the solution was atomized the recovery of the particles was poor. Particles were refreshed every other reservoir refill. The addition of the Tween 20[®] surfactant did not have an observable effect on the index of refraction, but there is a measured difference between the unmodified mil-prf-7024 and the working solution in this experiment. The pendant drop method was used to gather surface tension coefficient, 3 sets of 10 data points were taken on each of two samples. A paired t-test showed a statistically significant increase in surface tension after the addition of the surfactant and the particles. The difference in the mean of the 30 sample sets is 1.6%. A 1.6% deviation of surface tension equates to an increase in Webber number of 1.6% as well. This amount of deviation in Webber will not measurably affect the internal flow of the atomizer.

Density mismatch of the fluid and fluorescing particles can cause error in the data due to inertial effects causing the particle to incorrectly track the fluid streamlines. The Stokes number is the ratio of characteristic time of a fluid and a particle suspended in the fluid. Maintaining the Stokes number less than 1 (Raffel, Willert et al. 2007) ensures an error of less than 1% due to inertial effects of the particles.

Stokes number

$$Stk = \frac{t_o u_o}{l_o}$$

Particle characteristic
time

$$t_0 = \frac{\rho_d d_d^2}{18\mu_g}$$

u_o =Fluid velocity

l_o =Characteristic length

ρ_d =Particle density

d_d =Particle diameter

μ_g =Viscosity of fluid

The calculated stokes number for this flow was 0.18. The flow velocity used was the highest flow observed, 28 m/s. A characteristic length of .030 was used, representing the thickness of the fluid film in the cone area, and 9 micron particles were used in the study. The calculated Stokes number of less than 1 ensures that the density mismatch of the particles to the fluid was immaterial to the measurement error.

Results:

The average data plotted in contour plots is shown in Figure 20. Figure 18 displays the velocities at 207 kPa (30psi) from data taken at a 10 μ s time step and a 5 μ s time step. Figure 19 displays data taken at 621 kPa (90psi) and overlays data taken at a 5 μ s time step and a 2 μ s time step.

The research of (Xue, Jog et al. 2004) indicates the majority of mass transport in simplex atomizers occurs around the centerline. The data taken in this experiment agrees with this result. A range of time steps was studied with the shortest time steps proving most effective at resolving data close to the center, and longer time steps, up to 10 μ s, resolving velocities near the extremes of the measurement plane. At 207 kPa (30psi) the data taken at 10 μ s and 5 μ s correlate until the center of the atomizer where the 10 μ s data is absent. As Figure 18 shows, the 10 μ s data does

not provide additional information in the regions where the velocities are resolved. The same applies to the 5 μ s data set in the 621 kPa (90psi) experiment. In Figure 19 it can be observed that measured velocities are higher in the 621 kPa (90psi) test than the 207 kPa (30psi) test, further validating the data. The laser sheet which defines the imaging plane is approximately 1.0 mm (.040 in) offset from the centerline of the part in the direction of the camera. Due to the offset of the imaging plane, all of the data shows gaps in the orifice region, (Figure 20). In these data sets the orifice itself is out of the imaging plane. The data collected was susceptible to error due to problems in securing the camera relative to the test article through multiple tests. The imaging plane was sensitive to movement of the laser sheet, the test article and the camera focus. The in plane movement of the imaging plane is easily observed and measured in the image itself by referencing known features in the image such as the orifice. The through plane displacement measurement is less accurate, and was achieved by observing the air core at known displacements. Therefore the error in location of data collection is approximately ± 0.25 mm (0.01 in).

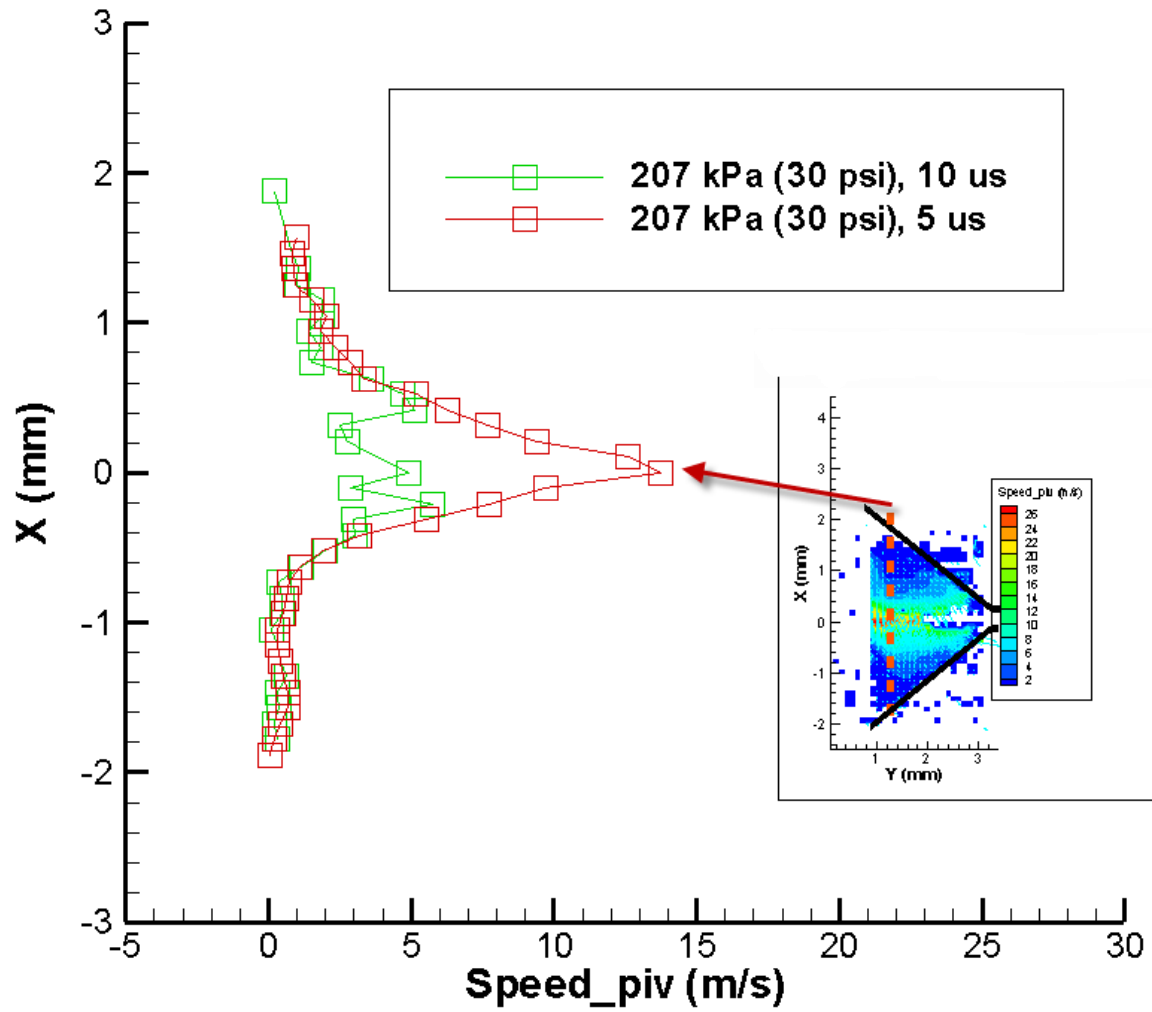


Figure 18: Velocity plots across the swirl chamber at a location close to the inlets. The 5 μ s and 10 μ s data matches very well until the center where the 10 μ s data shows a void. In this high speed region, the particles moved out of the laser sheet in between images leaving gaps in the data.

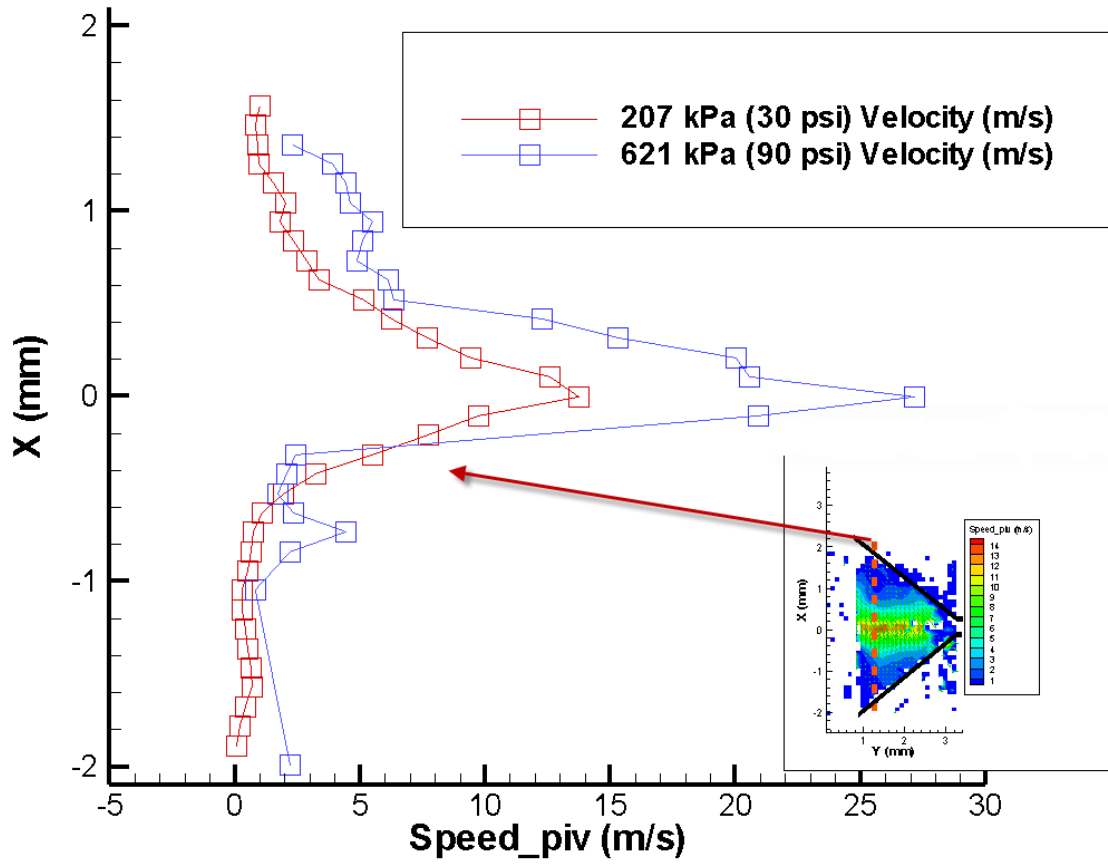
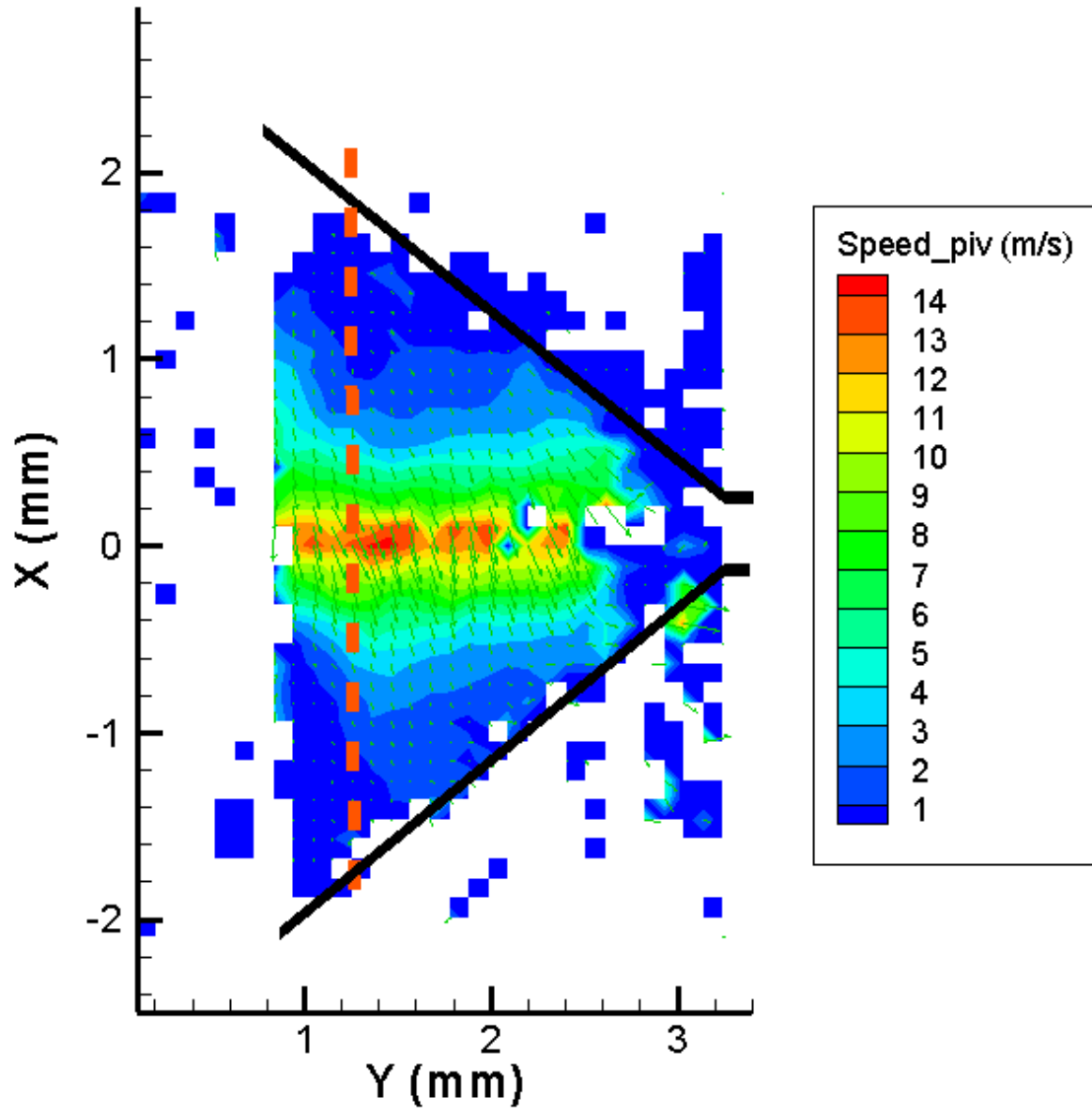


Figure 19: Velocity profile traverse at a location .762 mm (.030 in) down-stream of the swirl plug overlaid from the 207 kPa (30psi) set and the 621 kPa (90psi) set. The 621 kPa (90psi) data has the expected higher velocity. The 207 kPa (30psi) data is shifted to the left 50 pixels to account for a location change of the geometry.



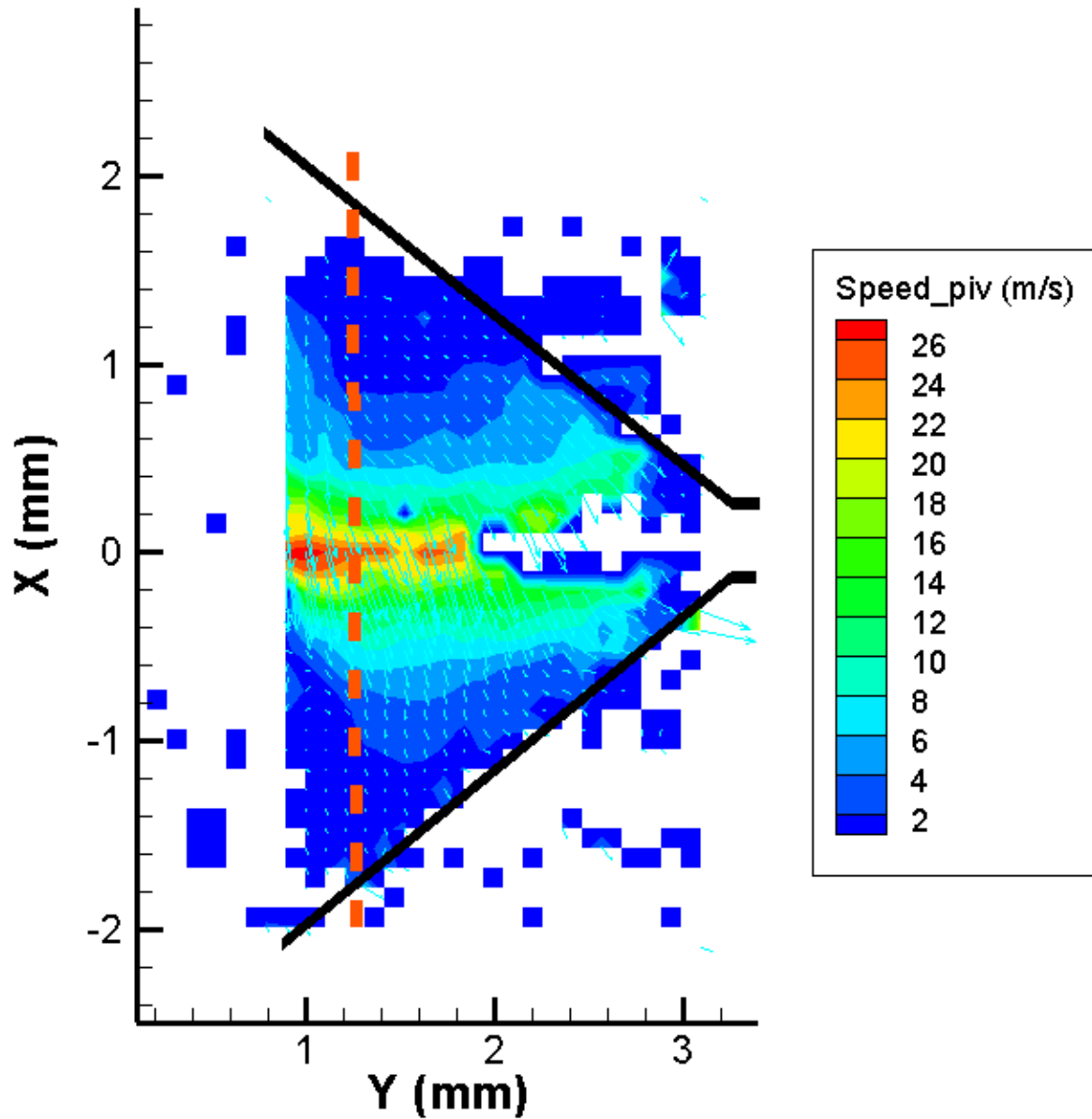
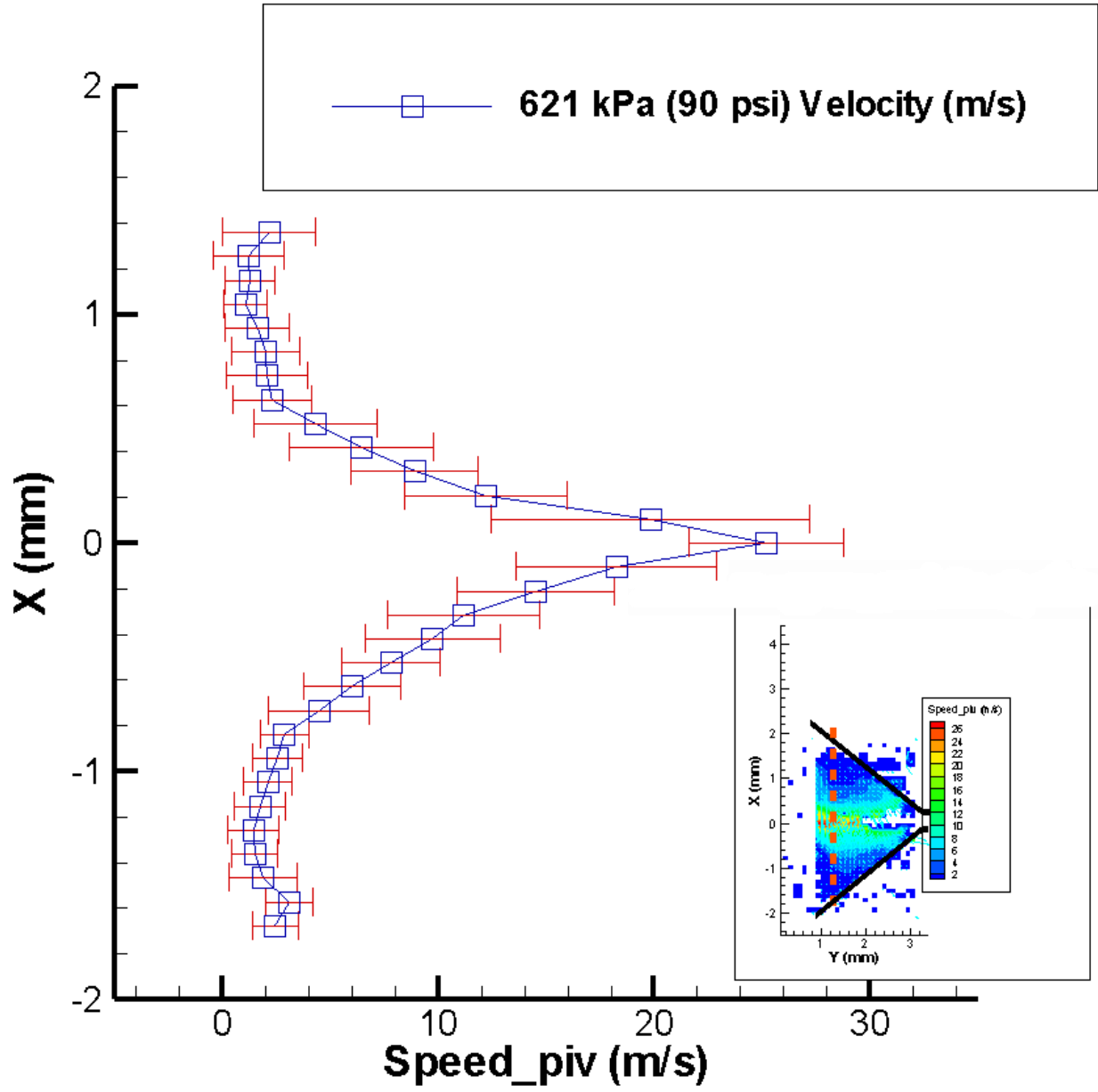


Figure 20: 207 kPa (30psi) and 621 kPa (90psi) data. Fuel flow is bottom to top with velocity vectors depicting significant flow right to left due to the planar offset of the data.

The error in the two laser pulses was verified during the zeroing of the laser plane offset using the tube. The laser was confirmed as illuminating the visible half of the tube at both exposures putting the error at less than 0.125mm (.005 in) total.



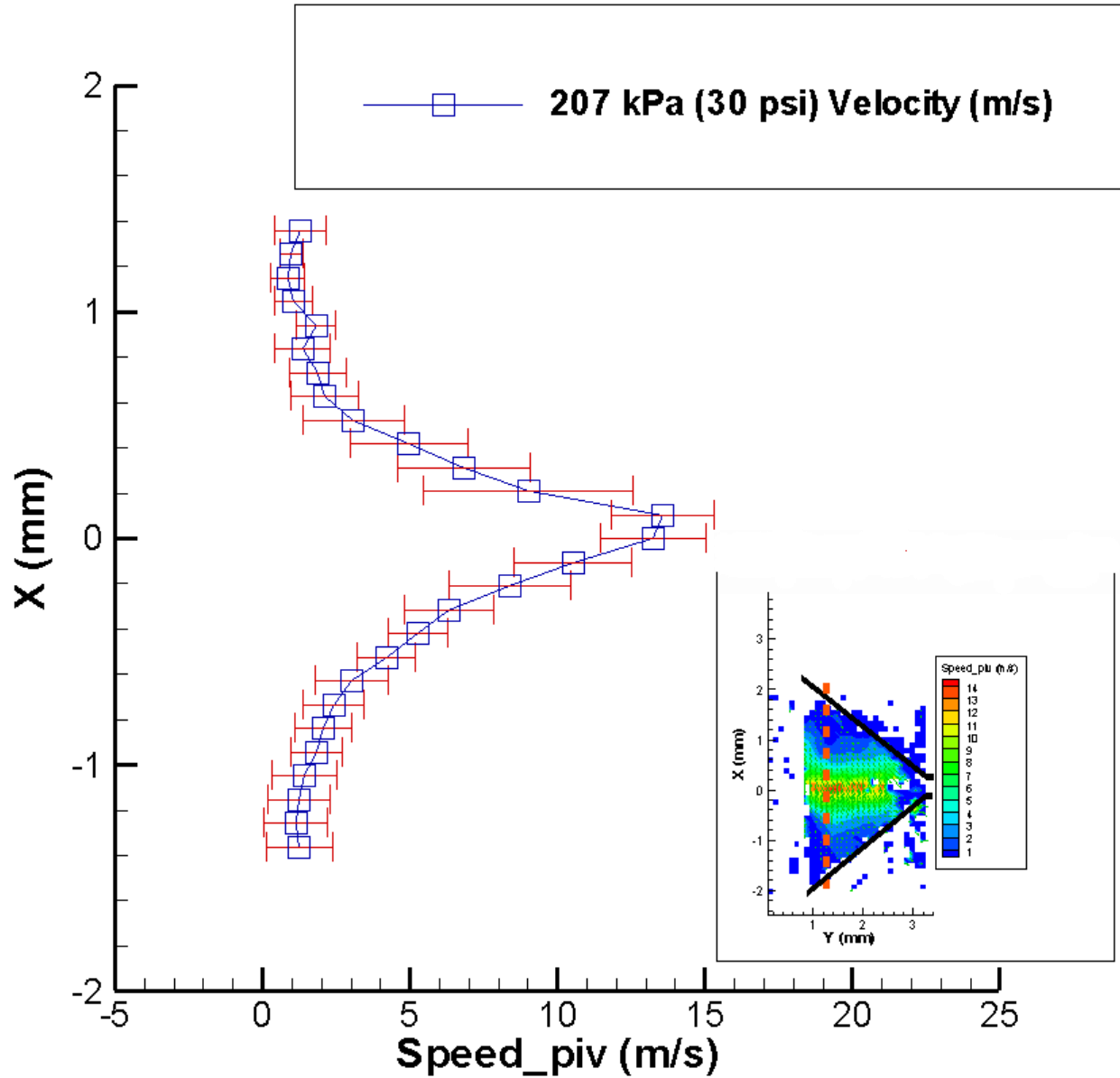


Figure 21: Positional velocity plots taken at the red line in the insert. The range over the data set is plotted in error bars.

Qualitative evaluation of the flow fields show a lack of definitive recirculation zones far from the centerline. This behavior has been measured in the idealized atomizers studied in the research of (Ma 2002)) and (Xue, Jog et al. 2004). This could be a measurement error due to the large velocity gradient between the center of the flow and the extreme radial locations. It is

Andy Thistle

likely a product of the axial component of the swirl plug not allowing recirculating flow structures to form. More study on the geometry studied here will add fidelity to this theory.

The flow data was taken 50 data points at a time, these image pairs were visually inspected to ensure the flow was on, all images of static and transient flows were discarded. The remaining images were processed using the WIDIM software package which outputs a range of velocities at a point as well as the average velocity. The average data is shown in figure 20, but the range can be seen in figure 21.

Andy Thistle

Conclusions:

The intent of this data set is to provide a baseline for future computational models of simplex atomizers in gas turbine fuel injection applications. Further research might involve taking data at a variety of planes at a parallel offset from the current data set. This data could function as further validation for a computational model. The computational model should be based on the geometry shown here. Once a functional model is identified, the methods can be applied to other geometries. The plane that is studied here is offset from the center of the atomizer in order to capture radial and axial flow data as well as to avoid the void caused by the air core. The pressure drops studied provide a wide range of mass flow and the data scales accordingly. The results of this research shows that PIV is a viable means of measuring velocities in sub-millimeter orifice simplex atomizers. Flow fields taken in this experiment qualitatively match past research on larger scale atomizers. The data from this experiment is available for further research at this link:

<https://dl.dropboxusercontent.com/u/5945622/Thistle-%20Measurement%20of%20Flow%20Velocities%20in%20a%20To-Scale%20Simplex%20Atomizer%20Using%20Particle%20Image%20Velocimetry%20Data.zip>

Works cited:

- (1997). PIV Hardware Operations Manual, TSI: 96.
- Baharanchi, A. A., M. Florida International University, FL, A. N. Darus, J. B. Technological University of Malaysia, Johor, Malaysia, M. Ansari, S. Islamic Azad University of Shahrood, Iran, E. A. Baharanchi and I. Islamic Azad University of Najafabad, Iran (2013). An Optimum Method of Capturing Interface and a Threshold Weber Number for Inclusion of Surface Tension Force in Simulation of Nozzle Internal Flow in Pressure Swirl Atomizers. ASME 2012 International Mechanical Engineering Congress and Exposition, American Society of Mechanical Engineers.
- Benjamin, M. A., R. J. Jensen and M. Arienti (2010). "REVIEW OF ATOMIZATION: CURRENT KNOWLEDGE AND FUTURE REQUIREMENTS FOR PROPULSION COMBUSTORS." **20**(6): 485-512.
- CFM. (2016). "CFM International, the World's Leading Aircraft Engine Manufacturer." from <http://www.cfmaeroengines.com/>.
- Dash, S. K., M. Peric, S. K. Som and M. R. Halder (2001). "Formation of Air Core in Nozzles With Tangential Entry." Journal of Fluids Engineering **123**(4): 829-835.
- GE (2014) "World's First Plant to Print Jet Engine Nozzles in Mass Production - GE Reports."
- Lefebvre, A. (1988). Atomization and Sprays, CRC Press.
- Lefebvre, A. H. and D. R. Ballal (2010). Gas Turbine Combustion: Alternative Fuels and Emissions, Third Edition, CRC Press.
- Ma, Z. (2002). Investigation on the internal flow characteristics of pressure-swirl atomizers. 3045306 Ph.D., University of Cincinnati.
- MIT. (2016). "3.7 Brayton Cycle." from <http://web.mit.edu/16.unified/www/SPRING/propulsion/notes/node27.html>.
- Raffel, M., C. E. Willert, S. T. Wereley and J. Kompenhans (2007). Particle Image Velocimetry: A Practical Guide (Experimental Fluid Mechanics), Springer.
- Robert W. Fox, P. J. P., Alan T. McDonald (2011). Fox and McDonald's Introduction to Fluid Mechanics [Book], Wiley.
- Scarano, F. (2001). WIDIM. Delft University of Technology: PIV Image Analysis Software.
- Steinhorsson, E., K. Ajmani, G. Tryggvason and M. Benjamin (1997). Numerical simulations of multi-fluid flows in fuel atomizers. Proceedings of the 1997 ASME Fluids Engineering Division Summer Meeting, FEDSM'97. Part 16 (of 24), June 22, 1997 - June 26, 1997, Vancouver, Can, ASME.
- Xue, J., M. A. Jog, S. M. Jeng, E. Steinhorsson and M. A. Benjamin (2004). "Effect of geometric parameters on simplex atomizer performance." AIAA Journal **42**(12): 2408-2415.
- Zeller, A. and S. Jayasekera (2014). PIV Post Processing.
- Zeller, A., S. Jayasekera, I. Dias and F. Scarano (2014). PIV_Processing.

Appendices:

	Dimension	English	Metric		Dimension	English	Metric
A	Orifice Diameter	.030"	.76mm	D	Injection port angle	55°	55°
B	Spin chamber OD	.130"	3.30mm	E	Injection port diameter	.021"	.53mm
C	Spin Chamber Angle	78°	78°	F	Injection port offset	.042"	1.07mm
				G	Angle of imaging plane	10°	10°

Table 4: Nominal dimensions for the test piece used. In addition to the injection port being offset from the centerline the hole centerline passes through a plane that is made of the centerline of the swirl plug and a point tangent to the hole, plane A. Plane A is normal to a plane B formed by the centerline of the injection port and the point tangent to the hole.

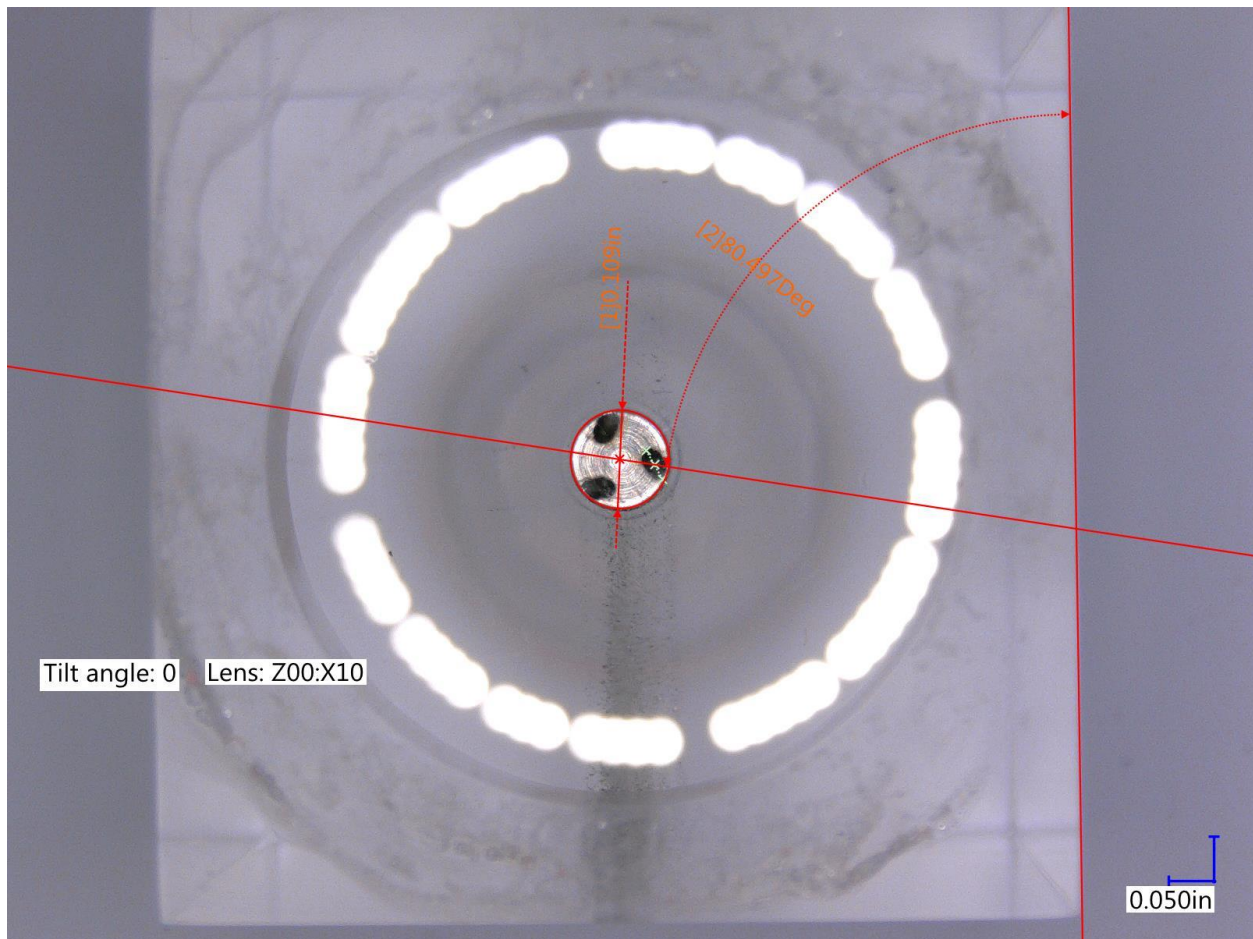


Figure 22: Experimental atomizer viewed at 10X directly through the orifice. The orientation of the swirl plug is shown overlaid. The index matching properties of the fluid and the atomizer allow this clear image to be viewed through the complex geometry of the atomizer. The experiments were performed with the laser sheet entering from left to right, fluid flowing out of the page and imaging with the camera mounted above the image.